

Estimation of effective parameters for the transition-metal complexes by mapping self-interaction correction onto GGA+U

Jae-Hyeon Park^{1,2, a)}

¹⁾*Interdisciplinary Program of Computational Science and Technology,
Seoul National University, Seoul 08826, Republic of Korea*

²⁾*Research Institute of Basic Sciences, Seoul National University, Seoul 08826,
Republic of Korea*

(Dated: 12 March 2020)

We propose a method to calculate the Hubbard U parameter in GGA+U or the α parameter in the atomic self-interaction correction (ASIC) scheme for transition-metal d orbitals by mapping the self-interaction correction (SIC) onto GGA+U, which is suitable for atom-centered basis sets. SIC can offer a substitute for the Hubbard U parameter in GGA+U, although its usage should be limited considering the differences between GGA+U and SIC. Approximations to reduce computational cost for self-interaction (SI) corrected localized orbitals are deduced from the properties of the unitary transformation in SIC and the atomic likeness of molecular orbitals dominated by transition-metal d orbitals, and the parameters are obtained from the approximate forms of the localized orbitals. First-row transition-metal complexes were tested, and the results are comparable to experimental measurements and previous calculations. Our method does not guarantee better results than those of the linear response method or hybrid functionals, but mapping from SIC suppresses overestimation of the U parameter to obtain proper geometries and energies for Fe-porphyrin-imidazole, Fe-porphyrin-CO and FeO₂ modeling.

^{a)}Electronic mail: parkq2@snu.ac.kr

I. INTRODUCTION

Transition-metal complexes have a wide range of applications, but the development of analysis tools can enhance their usage. These complexes have been widely used as catalysts, photosensitizers, and phosphors, and they can be used in the medical field¹⁻⁵ and environmental energy science.^{6,7} However, transition-metal complexes with a huge number of atoms (*e.g.*, myoglobin or hemoglobin) are difficult to analyze theoretically. The advancement of computational science is crucial to overcome such an obstacle. The development of low-cost algorithms is the best option if high-end computer facilities are not expected to be available.

Transition-metal compounds have influenced the development of quantum calculation methods. Density functional theory (DFT), first proposed by Hohenberg, Kohn, and Sham, has been quite successful in local density approximation (LDA) or generalized gradient approximation (GGA) applications. GGA provides good estimations of the geometries and energetics of molecules on atom-centered basis sets such as Gaussian orbital basis sets and linear-combinations-of-pseudo-atomic-orbital (LCPAO) basis sets.⁸⁻¹⁰ Although less accurate compared to coupled cluster methods or complete active space self-consistent field methods, DFT has the advantage of being less costly while providing reasonable accuracy levels.^{10,11} However, traditional DFT often produces inaccurate results for molecules with transition-metal or rare-earth atoms¹¹⁻¹⁹ because the self-interaction (SI) errors are considerable due to the *d* or *f* electron localization. Gradient correction of GGA cannot effectively reduce the SI errors because the traditional DFT is based on the delocalized electron picture. On the other hand, SI errors in transition-metal or rare-earth complexes can be eliminated by a method based on the localized electron picture. Various methods such as hybrid GGA^{20,21} and GGA+U²² have been proposed to merge the localized electron picture and the delocalized electron picture²³ and to correct SI errors.

GGA+U is one of the most commonly used methods for transition-metal complexes. It is a variation of LDA+U, which is LDA plus a correction composed of a Hubbard (mean-field or Hartree-Fock) term and a double-counting (DC) term,²⁴

$$E^{LDA+U}[\rho^\sigma(\mathbf{r}), \{n^\sigma\}] = E^{LSDA}[\rho^\sigma(\mathbf{r})] + E^{Hubbard}[\{n^\sigma\}] + E^{DC}[\{n^\sigma\}]$$

where E^{LSDA} is the LSDA (local spin density approximation. LDA with spin discrimination. In GGA+U, this is replaced by GGA.) functional and $\rho^\sigma(\mathbf{r})$ represents the electron

density for spin σ . The density matrix n^σ can be defined based on the Green function matrix on a localized orbital basis set²⁴ or from the local projections on Kohn-Sham (KS) orbitals.²⁵ The Hubbard term and the DC term in LDA+U have been determined by various formulations.^{24,26} A popular approach is the simplified LDA+U of Dudarev *et al.*²⁷

$$E^{LDA+U}[\rho^\sigma(\mathbf{r}), \{n^\sigma\}] = E^{LSDA}[\rho^\sigma(\mathbf{r})] + \frac{1}{2} \sum_I U_I \sum_\sigma \left[\sum_m n_{Imm'}^\sigma - \sum_{mm'} n_{Imm'}^\sigma n_{Imm'}^\sigma \right]$$

$$V^{LDA+U} = V^{LDA} + \sum_I U_I \sum_{mm'} \left[\frac{1}{2} \delta_{mm'} - n_{Imm'}^\sigma \right] \hat{P}_{Imm'}^\sigma. \quad (1)$$

In this equation, $I \equiv \{inl\}$ (i : atom index, n : principal quantum number, and l : azimuthal moment number), and $\hat{P}_{Imm'}^\sigma$ is the projector on $\{Imm'\}$ orbital (m, m' : magnetic moment indices). In addition, U_I , termed the on-site Coulomb interaction parameter or the Hubbard U parameter, was often determined empirically before linear response approaches were developed. It is a spherically averaged parameter in this version of LDA+U, which provides precise calculations if coordination environments are close to spherical symmetry. Because the correction terms in LDA+U incur only a low additional computational cost, LDA+U (or GGA+U) has been considered as one of the most efficient approaches in descriptions of large-scale correlated systems.²⁵

Applying to atom-centered basis sets can increase the efficiency of LDA+U calculations. Large-scale $O(N)$ LDA+U calculations can be realized on atom-centered basis sets,²⁵ meaning that very large transition-metal complexes can be analyzed by $O(N)$ GGA+U. However, there has been some controversy with regard to how the orbital occupations are defined on atom-centered basis sets.²⁸ Han *et al.* resolved this problem by introducing a ‘dual’ representation scheme.²⁵

$$\hat{P}_{Imm'}^\sigma = \frac{1}{2} (|\widetilde{Im'\sigma}\rangle \langle Im\sigma| + |Im'\sigma\rangle \langle \widetilde{Im\sigma}|) \quad (2)$$

where $|\widetilde{Im'\sigma}\rangle = \sum_{Jm'} S_{Im, Jm'}^{-1} |Jm'\sigma\rangle$ and $S_{Im, Jm'}$ is the overlap matrix. The dual representation obeys the sum rule for the total number of electrons.²⁵

In terms of accuracy, the improvement of the linear response method has enabled a precise estimation of the Hubbard U values. Pickett *et al.* was the first to introduce a linear response approach with constrained DFT.²⁸ It starts with an energy minimization equation,

$$E[\{q_I\}] = \min_{\rho(\mathbf{r}), \alpha_I} \left\{ E[\rho(\mathbf{r})] + \sum_I \alpha_I (p_I - q_I) - \mu \left(\int \rho(\mathbf{r}) d^3r - N \right) \right\}$$

where $E[\rho(\mathbf{r})]$ is the LDA+U functional, with the other variables being constraint terms. N is the total number of electrons, and p_I is the population on a group of orbitals with index I ($\equiv \{inl\}$),

$$p_I = \sum_{\sigma m} n_{Imm}^{\sigma}$$

and the Lagrange multipliers α_I can be interpreted as potential shifts for constraints of the population on I , $p_I = q_I$.²⁸ Slight change of q_I can give the formula of U_I in the differential definition,

$$U_I = \frac{\partial^2 E[\{q_I\}]}{\partial q_I^2} = -\frac{\partial \alpha^I}{\partial q_I}. \quad (3)$$

However, the constrained total energy involves a kinetic energy part²⁸ that causes inaccuracy during the U value calculations because the Hubbard U parameter is originally defined as having only the potential energy contribution. Cococcioni and de Gironcoli²⁹ subtracted the influence of the kinetic energy by adding so-called noninteracting KS term to Eq. (3),

$$U_I = \frac{\partial^2 E[\{q_I\}]}{\partial q_I^2} - \frac{\partial^2 E^{KS}[\{q_I\}]}{\partial q_I^2}$$

where

$$E^{KS}[\{q_I\}] = \min_{\rho(\mathbf{r}), \alpha_I} \left\{ E^{KS}[\rho(\mathbf{r})] + \sum_I \alpha_I^{KS} (p_I - q_I) - \mu \left(\int \rho(\mathbf{r}) d^3r - N \right) \right\}$$

or a response function form after Legendre transformation

$$U_I = (\chi_0^{-1} - \chi^{-1})_{II}$$

where $\chi_{IJ} = \frac{\partial p_I}{\partial \alpha_J}$, $\chi_{IJ}^0 = \frac{\partial p_I}{\partial \alpha_J^{KS}}$

They successfully applied this method to the transition-metal oxide solids and obtained greater accuracy levels when estimating the electronic and structural properties compared to those in earlier works.²⁹ The linear response approach has also been successful in calculations of pressure dependencies in the geometry³⁰ and spin states³¹ of transition-metal-containing perovskites and in estimations of the spin-state energetics in transition-metal complexes.^{16,22,32}

Nevertheless, the linear response method also has its limits. For instance, it can severely underestimate U values in closed-shell systems^{26,33} and can overestimate them for low-spin states.¹⁶ Zhao *et al.* indicated that these limits might be related to the local nature of the correction term in LDA+U³⁴ although using ultrasoft pseudopotentials could affect the U values.³⁵ On the other hand, the number of basis wavefunctions for the density response must be substantial in order to resolve density changes. For atom-centered basis functions, it is difficult to increase the number of basis orbital functions sufficiently because the Hubbard U parameters for multiple- ζ orbitals or polarization orbitals are not clearly defined²⁵ and many basis orbital functions lead to numerical instability due to the non-orthogonality arising in such cases.¹⁰ To the best of our knowledge, no one has published successful application of the linear response method to an atom-centered basis set as precise as that to a plane-wave basis set. Another method is necessary to estimate the U parameter in an atom-centered basis set.

Merging the localized electron picture and the delocalized electron picture is not the only solution available when dealing with SI errors. Self-interaction correction (SIC), introduced by Perdew and Zunger, refers to the direct subtraction of SI terms (from the LSDA or the GGA functional), representing a straightforward form of SIC to atoms in the early stage of DFT.³⁶ Two problems can arise when using the first version of the SIC method: non-orthogonality of the KS eigenfunctions and inconsistent results with regard to the symmetry of the system.³⁶ Non-orthogonality can easily be solved,³⁷ but the problem of inconsistency in the system requires much work, which long remained unexplored until research by Lin *et al.*, who found several breakthroughs.^{38–40} They defined what is known as ‘localized orbitals’ ϕ_j^σ , distinguished from (canonical) KS orbitals ψ_k^σ , and linked the localized orbitals with KS orbitals by unitary transformation $\psi_k^\sigma = \sum_j M_{kj}^\sigma \phi_j^\sigma$, leading to the construction of the

symmetry-consistent Hamiltonian.³⁷

$$H_k^\sigma \psi_k^\sigma = \sum_j \epsilon_{kj}^\sigma \psi_j^\sigma$$

$$H_k^\sigma = H_0 + \sum_j M_{kj}^\sigma v_{SIC,j}^{\phi,\sigma} \frac{\phi_j^\sigma}{\psi_k^\sigma}$$

where $v_{SIC,j}^{\phi,\sigma} = v_{Coulomb}(\rho_j; \mathbf{r}) + v_{XC}^\sigma(\rho_j^\uparrow, 0; \mathbf{r})$

$$v_{Coulomb}(\rho; \mathbf{r}) = \int d\mathbf{r}' \frac{\rho(\mathbf{r}')}{|\mathbf{r} - \mathbf{r}'|},$$

$$v_{XC}^\sigma(\rho^\uparrow, \rho^\downarrow; \mathbf{r}) = \frac{\delta E_{XC}[\rho^\uparrow, \rho^\downarrow]}{\delta \rho^\sigma(\mathbf{r})},$$

and ρ_j^σ is defined as $|\phi_j^\sigma|^2$. Here, $v_{Coulomb}$ is the electrostatic potential (also known as the Hartree potential), and v_{XC}^σ is the exchange-correlation potential. Their formulation pushed the boundary of SIC usage out of atomic calculations and has since been applied to several solid-state systems.³⁷

Aside from accuracy issues, it is important to reduce the large computational cost of SIC. Zunger⁴¹ and Rieger and Vogl⁴² proposed combining pseudo-potentials with SIC, where the complicated SIC energy minimization procedure is compacted into pseudo-potential generation,⁴² but the SIC contribution comes only from the core part, and neglecting the valence part does not reduce the computational cost much.³⁷ Vogel and colleagues^{43,44} include the valence SIC contribution by approximating the valence wavefunctions as atomic-like functions, which is the origin of the name of this method, ‘atomic SIC’ (ASIC). ASIC replaces the localized orbitals ϕ_j^σ with atomic orbitals Φ_{Im}^σ .

$$\sum_j v_{SIC,j}^{\phi,\sigma} \hat{P}_j^{\phi,\sigma} \rightarrow \sum_{Im} v_{SIC,Im}^{\Phi,\sigma} \hat{P}_{Im}^{\Phi,\sigma}$$

$$v_{SIC,Im}^{\Phi,\sigma} = v_{Coulomb}(\rho_{Im}^\Phi; \mathbf{r}) + v_{XC}^\sigma(\rho_{Im}^{\Phi,\uparrow}, 0; \mathbf{r})$$

$$\rho_{Im}^{\Phi,\sigma} = p_{Im}^\sigma |\Phi_{Im}^\sigma|^2$$

where p_{Im}^σ is the occupation of the atomic orbital Φ_{Im}^σ ,

$$p_{Im}^\sigma = \sum_k f_k^\sigma p_{Im,k}^\sigma. \quad (4)$$

Here, f_k^σ is the occupation number of the KS orbitals ψ_k^σ and $p_{Im,k}^\sigma = \langle \psi_k^\sigma | \hat{P}_{Im}^{\Phi,\sigma} | \psi_k^\sigma \rangle$. Filippetti and Spaldin⁴⁵ improved this, introducing a more efficient and more accurate ASIC potential by replacing the non-local operator $\hat{P}_{Im}^{\Phi,\sigma}$ with p_{Im}^σ and applying a relaxation effect

of the eigenvalues through multiplication by $1/2$. In addition, Pemmaraju et al.³⁷ extended the use of ASIC by replacing the factor $1/2$ with the parameter α .

$$\sum_{Im} v_{SIC,Im}^{\Phi,\sigma} \hat{P}_{Im}^{\Phi,\sigma} \rightarrow \alpha \sum_{Im} v_{SIC,Im}^{\Phi,\sigma} p_{Im}^{\sigma}$$

In this case, α must be less than or equal to 1 (the one-electron limit), and it has been determined empirically as 1 or $1/2$ (to the best of our knowledge), although polar covalent bonding can cause α to deviate from 1 or $1/2$. Naturally, ASIC can be applied to transition-metal systems, as molecular orbitals (MOs) from d electrons are often atomic-like orbitals and because most successful applications of ASIC deal with semi-core d orbitals.³⁷

Although ASIC and LDA+U have been developed independently, the formulations of both methods are equivalent to each other. Given that both methods adopt atomic orbitals, it is not difficult to prove the equivalence between ASIC and LDA+U using analogous expressions for atomic orbital energies.³⁷ After the density matrix $n_{Imm'}^{\sigma}$ is diagonalized, the density functional of the simplified version of LDA+U [Eq. (1)] becomes

$$E^{LDA+U} = E^{LSDA} + \frac{1}{2} \sum_I U_I \sum_{\sigma m} [n_{Im}^{\sigma} - (n_{Im}^{\sigma})^2]$$

where n_{Im}^{σ} are the eigenvalues of the density matrix. Note that $n_{Im}^{\sigma} = p_{Im}^{\sigma}$ if the dual projector [Eq. (2)] is used with the Mulliken population scheme. From this functional, the following form of the atomic orbital energy is gained:

$$\epsilon_{Im\sigma}^{LDA+U} = \frac{\partial E^{LDA+U}}{\partial n_{Im}^{\sigma}} = \epsilon_{Im\sigma}^{LSDA} + U_I \left(\frac{1}{2} - p_{Im}^{\sigma} \right). \quad (5)$$

The counter part for this in ASIC³⁷ is

$$\epsilon_{Im\sigma}^{ASIC} = \epsilon_{Im\sigma}^{LSDA} - \alpha p_{Im}^{\sigma} \langle \Phi_{Im}^{\sigma} | v_{SIC,Im}^{\Phi,\sigma} | \Phi_{Im}^{\sigma} \rangle. \quad (6)$$

Comparing Eqs. (5) & (6) leads to

$$p_{Im}^{\sigma} U_I = \alpha p_{Im}^{\sigma} \langle \Phi_{Im}^{\sigma} | v_{SIC,Im}^{\Phi,\sigma} | \Phi_{Im}^{\sigma} \rangle$$

if the shift $\bar{U}_I/2$ in Eq. (5) is ignored.⁴⁶ This equation should be rearranged because U_I must be a parameter averaged over index m . Furthermore, p_{Im}^{σ} should be the weight in averaging, consistent with the spirit of SIC which counts only occupied states. Thus, it is necessary to

replace U_I in the equation above with U_{Im} to obtain

$$\begin{aligned}
 U_I &= \frac{\sum_{\sigma,m} p_{Im}^\sigma U_{Im}}{\sum_{\sigma,m} p_{Im}^\sigma} \\
 &= \alpha \frac{\sum_{\sigma,m} p_{Im}^\sigma \langle \Phi_{Im}^\sigma | v_{SIC,Im}^{\Phi,\sigma} | \Phi_{Im}^\sigma \rangle}{\sum_{\sigma,m} p_{Im}^\sigma}.
 \end{aligned}
 \tag{7}$$

The parameter α can be obtained from the relationship between the ϕ orbitals and the Φ orbitals. Thus, it is possible to estimate α corresponding to the transition-metal d orbitals if one finds an approximate form of the localized orbitals ϕ for the d orbitals. In such case, an approximate U value can be obtained from the above formula. This U value does not coincide with the original meaning of the Hubbard U parameter, but the one-electron limit ($\alpha = 1$) reduces the probability of overestimation. The methodology section explains how the localized orbitals ϕ can connect with the atomic orbitals Φ and how suitable the U values from SIC are to molecules calculated within GGA on an atomic orbital basis set.

In this paper, we propose a method to estimate the Hubbard U parameter or the α parameter for a transition-metal d orbital by exploiting the relationship between GGA+U and ASIC. This method will be useful for DFT calculations on atom-centered basis sets which have advantages of efficiency and an intelligible atomic analysis. Some approximations in this method are justified due to the characteristics of SIC for transition-metal complexes. It is shown that its application to simple molecules after describing the implementation procedure and computational details. From test results on simple molecules, the proposed method is assessed by comparing its results with those of the linear response method, and the limitations of the proposed method are discussed. Finally, suggestions for improvement are offered before summarizing the paper.

II. METHODOLOGY

A. Availability of the Hubbard Parameter Using SIC

The previous section described how the parameter U in GGA+U is closely related to the parameter α in ASIC, leaving the question of how similar U values estimated by SIC are to the original meaning of U . The atomic orbital SI energy can be decomposed into the Hartree electrostatic energy (the Coulomb term) and the exchange-correlation energy (the XC term). Likewise, the screened on-site Coulomb interaction or the Hubbard U parameter

can be decomposed into the bare Coulomb energy of pure atomic orbitals (identical to the Coulomb term in the SI expression) and the renormalizing terms of the exchange effect, the screening effect, and the orbital relaxation effect. One example of this is the expression of Solovyev and Dedrichs⁴⁷ although they ignored the exchange effect. The renormalizing terms in the expression for the Hubbard U are partially equivalent to the XC term in the SI expression, especially for molecular calculation within GGA. GGA provides the exchange effects and the screening effect under the charge-neutrality condition, making it suitable for molecules. The orbital relaxation effect is an analogy to the slight delocalization caused by a change of the atomic orbital if one replaces the atomic orbital Φ with the SIC localized orbital ϕ during the calculation of the atomic SI energy. The renormalizing terms in GGA+U have analogical counterparts in SIC with GGA. Hence, SIC can be used to estimate a substitute of the Hubbard U parameter on account of the similarity and equivalence between GGA+U and ASIC.

Of course, the use of substitute U parameters should be limited. Because the original meaning of the Hubbard U parameter includes the possibility of charge excitation in Mott insulators,⁴⁸ GGA+U is established to manage unoccupied states as well. On the other hand, SIC (or ASIC) considers only occupied states, meaning that SIC cannot consider occupation changes caused by excitation or the influence of unoccupied states. Thus, the substitute U value obtained from SIC should be used when a molecular system has a sufficiently large HOMO-LUMO gap or when the system is in a stable or a metastable state. Calculation of the ground state of the molecular system requires only the large HOMO-LUMO gap condition, but the excited states to be calculated require metastability as well. Therefore, the U parameter by SIC is available if the objective state of the complex system is stable and has a HOMO-LUMO gap of the order of 1 eV (usually larger than thermal fluctuations).

B. Assumptions of the Proposed Method

This study considers calculations for transition-metal complex molecules within GGA+U on an atom-centered basis set. Calculations based on an atom-centered basis set are known to have a limit of accuracy due to nonorthogonality¹⁰ in comparison to planewave based calculations, which means that the parameters U and α calculated on an atom-centered basis set frequently do not need to be as precise as when they are calculated on a planewave

basis set. This tolerance with regard to accuracy allows approximations for estimations of the parameters α and U instead of a rigorous calculation. MOs dominated by transition-metal d orbitals remain atomic-like unless they are considerably hybridized or widely conjugated, which can be satisfied when each transition-metal atom is isolated from the other transition-metal atoms. Here, ‘atomic-like’ means that the MOs almost hold the symmetries of the transition-metal d orbitals (the MOs do not need to be confined in an atom). The atomic likeness can be a key to the formation of suitable approximations.

Because the full calculation of SIC incurs a large computational cost and is not feasible, an approximation is necessary to obtain the localized orbitals ϕ for estimations of the parameters U and α . The ϕ orbitals related to transition-metal d orbitals are not far from the atomic orbitals Φ if the MOs corresponding transition-metal d orbitals are atomic-like. According to the ligand field theory, these MOs depend on the ligand coordination. Accordingly, it is assumed here that if the atomic orbitals Φ_I^σ of a transition-metal atom I are determined by ligand coordination (for example, $d_{x^2 - y^2}$, d_{xy} , d_{z^2} , and two d_π ’s for square pyramidal coordination,^{16,49}) an atomic orbital Φ_{Im}^σ has a corresponding localized orbital ϕ_j^σ in SIC, in one-to-one correspondence. One must reconstruct the atomic Φ_I^σ orbitals in accordance with the ligand coordination because the original atomic orbitals, *i.e.*, the Φ_I^0 orbitals provided by DFT packages), are constructed in an independent atom.

A clue to another approximation can be found from the unitary transformation in SIC (transformation from localized orbitals ϕ to canonical KS orbitals ψ , or vice-versa), which satisfies the sum rule

$$\sum_j |M_{kj}^\sigma|^2 = \sum_k |M_{jk}^\sigma|^2 = 1 \quad (8)$$

as a property of unitary transformations. The populations of KS orbitals projected onto localized orbitals also satisfy a sum rule in a form similar to that of M_{jk}^σ ,

$$\sum_j \tilde{p}_{j,k}^\sigma = \sum_k \tilde{p}_{j,k}^\sigma = 1 \text{ where } \tilde{p}_{j,k}^\sigma = \langle \psi_k^\sigma | \hat{P}_j^{\phi,\sigma} | \psi_k^\sigma \rangle$$

where the ϕ orbitals are obtained from SIC. In fact, one can easily prove that

$$\tilde{p}_{j,k}^\sigma = |M_{kj}^\sigma|^2,$$

which suggests that the unitary transformation is related to the orbital occupations. At this point, the unitary transformation can be written as

$$M_{jk}^\sigma = (\tilde{p}_{j,k}^\sigma)^{1/2} \exp(i\theta_{jk}^\sigma). \quad (9)$$

where $\exp(i\theta_{jk}^\sigma)$ is a phase factor. Given that the arguments here are restricted to molecular calculations, M_{jk}^σ can be constrained to real numbers because the eigenstates in the non-periodic boundary condition can be real wavefunctions. Thus, we can set $\exp(i\theta_{jk}^\sigma) = 1$ or -1 .

C. Main Approximations

The starting point is to approximate $\tilde{p}_{j,k}^\sigma$ in Eq. (9) because the exact estimation of $\tilde{p}_{j,k}^\sigma$ means full calculation of SIC. We assume that if a localized orbital ϕ_j^σ has one-to-one correspondence with an atomic orbital Φ_{Im}^σ , $\tilde{p}_{j,k}^\sigma \propto f_k^\sigma p_{Im,k}^\sigma$, where f_k^σ comes from the fact that a localized orbital ϕ_j^σ (SI corrected orbital) stems from occupied orbitals. Recall that $p_{Im,k}^\sigma$ is obtained from Φ_{Im}^σ . Because the sum rule (8) must be satisfied,

$$\tilde{p}_{j,k}^\sigma \approx f_k^\sigma p_{Im,k}^\sigma / p_{Im}^\sigma$$

due to the definition of p_{Im}^σ [Eq. (4)]. Thus, the unitary transformation (9) is approximated as

$$M_{jk}^\sigma \approx \frac{1}{\sqrt{N}} \left(\frac{f_k^\sigma p_{Im,k}^\sigma}{p_{Im}^\sigma} \right)^{1/2} \exp(i\theta_{jk}^\sigma), \quad (10)$$

where N is a normalization constant. Remember that this equation holds only if MOs are atomic-like and the Mulliken population scheme with the dual projector [Eq. (2)] should be used for the calculation of $p_{Im,k}^\sigma$ to satisfy the sum rule (8) if Φ_{Im}^σ orbitals are not generally orthogonal. Applying Eq. (10), one can obtain ϕ orbitals from the above unitary transformation,

$$\phi_j^\sigma = \sum_k (M^\sigma)_{jk}^* \psi_k^\sigma \approx (1/\sqrt{N}) \sum_k \left(\frac{f_k^\sigma p_{Im,k}^\sigma}{p_{Im}^\sigma} \right)^{1/2} \exp(-i\theta_{jk}^\sigma) \psi_k^\sigma. \quad (11)$$

Once the localized orbitals ϕ are obtained, to estimate the parameter α , it is necessary to introduce the concept by which α varies for different orbitals while ASIC uses an averaged α . The SIC energy of a localized orbital ϕ_j^σ can be decomposed into the SIC energy levels of Φ atomic orbitals.

$$\sum_{Jm'} \alpha_{Jm',j} p_{Jm'}^\sigma \langle \Phi_{Jm'}^\sigma | v_{SIC,Jm'}^{\Phi,\sigma} | \Phi_{Jm'}^\sigma \rangle = \langle \phi_j^\sigma | v_{SIC,j}^{\phi,\sigma} | \phi_j^\sigma \rangle.$$

Here, $\alpha_{Jm',j}$ can be interpreted as a coefficient of each SIC energy level for $\Phi_{Jm'}^\sigma$, and $\alpha_{Jm',j}$ corresponds to U_J . In addition, a portion of the right-hand side corresponding to the term

with $\alpha_{Jm',j}$ on the left-hand side can be approximately $q_{J,m'}^{j,\sigma} = \langle \phi_j^\sigma | \hat{P}_{Jm',\sigma}^\Phi | \phi_j^\sigma \rangle$ for consistency with the sum rule $\sum_{Jm'} q_{J,m'}^{j,\sigma} = 1$. At this stage, it becomes possible to set $\alpha_{Im,j} = \alpha_{Im}$ and $j = j(I, m)$ by applying the assumption of one-to-one correspondence between the Φ_{Im}^σ and the ϕ_j^σ for the transition-metal d . Thus,

$$\alpha_{Im} p_{Im}^\sigma \langle \Phi_{Im}^\sigma | v_{SIC,Im}^{\Phi,\sigma} | \Phi_{Im}^\sigma \rangle \approx q_{I,m}^{j(I,m),\sigma} \langle \phi_{j(I,m)}^\sigma | v_{SIC,j(I,m)}^{\phi,\sigma} | \phi_{j(I,m)}^\sigma \rangle, \quad (12)$$

which also results in the inequality

$$p_{Im}^\sigma \langle \Phi_{Im}^\sigma | v_{SIC,Im}^{\Phi,\sigma} | \Phi_{Im}^\sigma \rangle \geq q_{I,m}^{j(I,m),\sigma} \langle \phi_{j(I,m)}^\sigma | v_{SIC,j(I,m)}^{\phi,\sigma} | \phi_{j(I,m)}^\sigma \rangle \quad (13)$$

because $\alpha_{Im} \leq 1$. Note that the approximation (12) emerges due to the approximate nature of GGA+U (or LDA+U). It is necessary to apply Eq. (11) to GGA+U because we cannot obtain all localized orbitals ϕ_j^σ within the condition of atomic likeness and GGA+U requires only a few U values for atomic-like MOs. We would need another kind of approximation instead of (12) if we replace GGA+U with another method.

The effective Hubbard U value for transition-metal d can be obtained from Eqs. (7) & (12)

$$U_I \approx \frac{\sum_{\sigma,m} q_{I,m}^{j(I,m),\sigma} \langle \phi_{j(I,m)}^\sigma | v_{SIC,j(I,m)}^{\phi,\sigma} | \phi_{j(I,m)}^\sigma \rangle}{\sum_{\sigma,m} p_{Im}^\sigma}. \quad (14)$$

This equation and Eq. (12) result in α_I , the average of α_{Im} ,

$$\alpha_I = \frac{\sum_{\sigma,m} q_{I,m}^{j(I,m),\sigma} \langle \phi_{j(I,m)}^\sigma | v_{SIC,j(I,m)}^{\phi,\sigma} | \phi_{j(I,m)}^\sigma \rangle}{\sum_{\sigma,m} p_{Im}^\sigma \langle \Phi_{Im}^\sigma | v_{SIC,Im}^{\Phi,\sigma} | \Phi_{Im}^\sigma \rangle}. \quad (15)$$

Note that a direct comparison of the Hamiltonians, which provides the exact expression for α_I , is not used for this expression. One can find clues about the precise expression in the literature,⁴⁶ but an accurate calculation of α_I will incur an excessively high computational cost without approximations.

D. Implementation

To implement the proposed idea, one must construct atomic orbitals Φ_I^σ as linear combinations of the original atomic orbitals Φ_I^0 . The regenerated atomic orbitals Φ_I^σ should be well matched with the symmetry stemming from the degree of ligand coordination. If an atomic

orbital Φ_{Im}^σ has one-to-one correspondence with a localized orbital ϕ_j^σ , the canonical KS orbitals which compose the ϕ_j^σ via the unitary transformation (10) can form a group because the KS orbitals should be related to Φ_{Im}^σ . Thus, each atomic orbital Φ_{Im}^σ of transition-metal d has a group of KS orbitals. It is therefore assumed that a KS orbital in a group does not participate in the localized orbitals corresponding to the other groups during the unitary transformation due to the atomic likeness. Accordingly, one should classify KS orbitals into groups related to the (transition-metal d) atomic orbitals Φ_I^σ . There are two ways to classify KS orbitals. The first is to check the expansion coefficients of KS orbitals expanded on the original atomic orbitals Φ_{Im}^0 ,⁵⁰ and the second is to analyze the relative coordinates and ligand species. In either case, at least one symmetry axis should coincide with one of the coordinate axes in order to reduce the numerical complexity. Our classification algorithm is comparing the expansion coefficients of the KS orbitals.

The next step is an adjustment of the phase factors, which completes the localized orbitals of characteristics of transition-metal d . Each KS orbital is assigned to a group corresponding to an atomic orbital Φ_{Im}^σ during the previous step. The phase factors of M_{jk}^σ should be consistent in each group. Fortunately, in a non-periodic boundary condition, the phase factors can be restricted to 1 or -1. In the algorithm here, for the determination of the phase factors, elements of M_{jk}^σ in the row of index j should be sorted by the absolute value $|M_{jk}^\sigma|$. Next, the signs of M_{jk}^σ from the smallest $|M_{jk}^\sigma|$ to the largest should be varied in order to maximize the SI energy of the localized orbital ϕ_j under the condition of inequality (13).⁵¹

The final step is to calculate the effective Hubbard U value. This can be done by dividing it into the Coulomb term and the XC term for each localized orbital; these terms can be calculated by expanding each localized orbital on real grids.⁵² After calculation of the SI energy for each localized orbital, it is necessary to follow Eq. (14). First, one should summate the SI energies of all orbitals multiplied by the projected populations $q_{I,m}^{j(I,m),\sigma}$, with the summed value then divided by the total population $\sum_{\sigma,m} p_{Im}^\sigma$.

E. Computational Details for Tests

DFT calculations were performed on the geometric and magnetic structures of simple transition-metal complexes. These calculations were within the GGA+U framework with the PBE exchange-correlation functional⁵³ and were done with the OpenMX package⁵⁴ based

on the method of LCPAO.⁵⁰ The chosen pseudo-atomic orbitals were (in OpenMX notation) Ti9.0-s2p2d1, Fe8.0S-s3p2d1, Ni8.0H-s4p3d1, C7.0-s2p2d1, O6.0-s2p2d1, N6.0-s2p2d1, and H6.0-s2p1, generated on Troullier-Martins norm-conserving pseudopotentials⁵⁵ in Blochl separable form⁵⁶ with partial core correction.⁵⁷ We cannot consider more than single- ζ basis orbitals for the d orbitals because the Hubbard U values for multiple- ζ orbitals or polarization orbitals are not yet clearly defined. The real grid technique⁵² with an energy cutoff value of 300 Ry was applied to calculation of the Coulomb and exchange-correlation parts. The criterion of self-consistent field energies was chosen as 1×10^{-7} hartree, while the force criterion was 4×10^{-4} hartree/bohr to optimize all of the structures. Binding energies were calculated with counterpoise correction.⁵⁸

III. TEST RESULTS

A calculated U value is a result obtained by a GGA+U calculation with an input U value. In the linear response method, the output U values should be calculated for consistent states, as emphasized by Kulik *et al.*²² This is also in good agreement with the philosophy of SIC, which implies that in the proposed method, SI errors must be properly removed when the output U value is identical to the input U value, *i.e.*, the U parameter is obtained in a self-consistent manner. Hence, here the resulting U values have less discrepancy from the input U value than 0.1 eV. With this criterion, several simple molecules were tested, Fe-porphyrin-imidazole, Fe-porphyrin-CO, FeO₂, and transition-metal monoxide molecules. The Hubbard U values of these molecules are compared with the linear response calculations on planewave basis sets.^{16,32,59} We also compare geometric and energetic results with those of hybrid functionals and wavefunction theories as well as those of the linear response method.

A. Iron Porphyrin Imidazole

This molecule is also known as five-coordinated deoxyheme (Fig. 1), an important simplified model to explain the physiological mechanisms of myoglobin and hemoglobin, but the DFT calculation of five-coordinated iron is so demanding that GGA and restricted B3LYP predict incorrect ground states.¹⁶ GGA+U was proposed as a feasible remedy and offered correct ground states for five-coordinate Fe-porphyrin complexes.¹⁶ The spin state of Fe-

TABLE I. The calculated U values of the Fe $3d$ orbitals (eV) for two states of iron porphyrin imidazole within the proposed method (U^{SIC} . Corresponding α in parentheses) and the previous linear response calculation (LR¹⁶)

state	U^{SIC}	LR
${}^5B_{2g}$	4.2 (0.88)	3.9
3E_g	3.7 (0.78)	-
Average	4.0 (0.83)	-

porphyrin-imidazole is experimentally known to be a ferrous high spin state where six d electrons are distributed to five d characteristic MOs on four energy levels (*i.e.*, two MOs are degenerate) according to the ligand field theory.⁴⁹ GGA+U determines the ground state as the ferrous high spin state of ${}^5B_{2g}$ [$(d_{xy})^2(d_{\pi})^2(d_{x^2-y^2})^1(d_{z^2})^1$] while GGA provides the ferrous intermediate spin state of 3E_g [$(d_{xy})^2(d_{\pi})^3(d_{z^2})^1$] as the ground state. The Fe d configuration of our GGA+U ground state is consistent with that of the unrestricted B3LYP ground state.⁶⁰

Our calculations for this molecule agree with the previous linear response calculation on a planewave basis set. As shown in Table I, 4.2 eV was obtained as the U value for ${}^5B_{2g}$, close to the U value 3.9 eV by the previous linear response calculation,¹⁶ and the U value for 3E_g was found to be 3.7 eV. With the average U value over the two states, 4.0 eV, the ground state was identified to be the ${}^5B_{2g}$ state and the energy difference from the ground state to the excited state 3E_g was identified to be 0.21 eV, close to the previous calculations such as the linear response result of 0.21 eV¹⁶, the unrestricted B3LYP result of 0.3 eV⁶⁰, and the CCSD(T) result of 0.13 eV.⁶¹ The estimated α values for ${}^5B_{2g}$ and 3E_g were 0.88 and 0.78, respectively, showing little deviation from the empirical α value for molecules, 1.³⁷ The ${}^5B_{2g}$ geometry is in agreement with those of the linear response and the experimental measurement, where the out-of-plane displacement of the iron atom ($d_{\text{Fe-por}}$) strongly depends on the spin state, as shown in Table II. A Mulliken analysis revealed that the iron atom determines the spin state of the molecule and that its d electron configuration is in general agreement with the previous calculation.¹⁶

TABLE II. Geometric parameters (\AA) for Fe-porphyrin-imidazole in this study (GGA and GGA+U), compared with the previous calculations (LR and UB3LYP) and the experiments (Exp.)

	$d_{\text{Fe-Por}}$	Fe-N_{por}	Fe-N_{Im}
GGA 3B_2	0.12	2.00	2.25
GGA+U 3B_2	0.12	2.03	2.38
GGA+U 5B_2	0.38	2.11	2.21
LR ^a	0.43	2.11	2.19
UB3LYP ^b	0.43	2.11	2.19
Exp. ^c	0.363	2.07	2.14
Exp. ^d	0.31	2.075	2.134
Exp. ^e	0.42	2.06	2.1

^a GGA + U ($U = 3.9$ eV), Ref. 16

^b Ref. 59

^b Ref. 62

^c Ref. 63

^d Ref. 64

B. Iron porphyrin carbon monoxide

This molecule, also known as five-coordinated carboxyheme (Fig. 2), can serve as a model for investigating the mechanisms of CO gas sensors.⁶⁵ Because the CO molecule is a strong ligand, the iron atom becomes the ferrous low spin state.⁴⁹ Conventional DFT methods provide the ferrous low spin state of this system^{66–68} in agreement with experimental results, but they overestimate the CO binding energy.⁶⁹ Thus it is expected that GGA+U can improve the calculation of the CO binding energy, but the linear response method provided the incorrect spin state for this molecule due to the overestimated U value.¹⁶

Our calculations for Fe-porphyrin-CO are consistent with experimental observations. Table III shows the estimated Hubbard U values for the two states, the ferrous low spin ${}^1A_{1g}$ [$(d_{xy})^2(d_{\pi})^4$] and the ferrous intermediate spin 3E_g [$(d_{xy})^2(d_{\pi})^3(d_{z^2})^1$]. Their corresponding α values (0.59 and 0.64, respectively) are closer to 1/2 than 1 and are good examples of significant deviation from the empirical α value for molecules. With the average U value, 2.9 eV, we identified the ground state to be ${}^1A_{1g}$ and the energy difference with

TABLE III. The calculated U values of the Fe $3d$ orbitals (eV) for two states of iron porphyrin carbon monoxide within the proposed method (U^{SIC} . Corresponding α in parentheses) and the previous linear response calculation (LR¹⁶).

state	U^{SIC}	LR
$^1A_{1g}$	2.7 (0.59)	7.2
3E_g	3.0 (0.64)	-
Average	2.9 (0.62)	-

TABLE IV. Bond lengths (\AA) and bond angles ($^\circ$) for Fe-porphyrin carbon monoxide in this study (GGA and GGA+U), compared with the previous calculations (Pre. 1¹⁶ and Pre. 2⁷¹) and the experiments (Exp.⁷³)

	Fe-C(CO)	Fe-N _{por}	C-O	Fe-C-O
GGA $^1A_{1g}$	1.68	2.00	1.20	180
GGA+U $^1A_{1g}$	1.72	2.02	1.19	180
GGA+U 3E_g	2.31	2.02	1.17	146
Pre. 1 ^a	1.77	2.01	1.12	-
Pre. 2 ^b	1.694	-	1.165	180
Exp.	1.77	2.02	1.12	179

^a GGA + U ($U = 5.0$ eV)

^b OLYP

the excited state 3E_g to be 0.27 eV, close to a CCSD(T) result of 0.28 eV.⁷⁰ A Mulliken analysis found that the iron atom dominates the magnetic moment of the molecule, as Fe-porphyrin-imidazole does. The CO binding energy in the ground state for the U value of 2.9 eV was computed as 0.49 eV, closer to the experimental value of 0.69 eV⁶⁹ than several hybrid functional results (0.281.8 eV)⁷¹ and a CCSD(T) result of 1.9 eV⁷⁰ although a CASPT2 binding energy, 0.69 eV,⁷² looks more accurate. Our GGA+U geometry for the low-spin state improved when compared to the GGA geometry and is close to an OLYP geometry (Table IV).

C. Iron Dioxide

In contrast to the previous two molecules, there are only two surrounding ligand atoms in this molecule, ensuring that the iron atom’s neighbor environment is not close to spherical symmetry, whereas the degree of deviation of the Fe d electrons from the atomic center might not be considerable. The bonding characteristic between a transition-metal atom and an oxygen atom is polar covalent, which can be represented as $\text{O}^{-2+\delta}\text{-Fe}^{+4-2\delta}\text{-O}^{-2+\delta}$. In addition, the $d_{x^2 - d_{y^2}}$ and the d_{xy} orbitals, which show nonbonding characteristics in the linear stick structure, contribute to the bending of FeO_2 by hybridizing with oxygen p orbitals.⁵⁹ Many meta-stable states hinder a search of the ground state, and a calculation of transition-metal dioxide molecules requires consideration of the change of the spin state and the geometric structure.

Two low-lying states were found, *i.e.*, the ferrous high spin state 5B_2 and the ferrous intermediate spin state 3B_1 , in the bent structures. As shown in Table V, the estimated U values for the two states were identified to be 3.3 eV for 5B_2 and 3.0 eV for 3B_1 , much lower than the previous linear response U values which were supposedly overestimated.⁵⁹ However, the energy difference between 5B_2 and 3B_1 for the average U value 3.2 eV was determined to be approximately 0.13 eV, close to the previous linear response result.⁵⁹ The α values were found to be 0.69 for 5B_2 and 0.64 for 3B_1 , closer to 1/2 than to 1, which is another example of considerable deviation from the empirical α value for molecules. A Mulliken analysis revealed that the Fe atomic spin moments in the both states with the proposed method are very similar in terms of magnitude and direction while the O atomic spin moments have opposite directions, indicating that the spin direction of the oxygen atoms can substantially controls the spin state of the molecule.

Our geometry appears reasonable and comparable to those of the linear response method⁵⁹ and quantum Monte Carlo (QMC).⁷⁴ Despite the difference in the estimated U values, bond lengths by the proposed method and the linear response method (GGA+U and LR in Table VI) are similar to each other, although they are slightly larger than the QMC bond length. The O-Fe-O bond angles show considerable dependence on the U value and the spin state, but our ground state (3B_1) bond angle is close to the experimental value and the QMC result. In the paper which undertook a calculation by the linear response method,⁵⁹ the researchers insisted that correction by an intersite interaction V plays an important role, and they

TABLE V. The calculated U values of the Fe $3d$ orbitals (eV) for two states of FeO₂ within the proposed method (U^{SIC} . Corresponding α in parentheses) and the previous linear response calculation (LR⁵⁹).

state	U^{SIC}	LR
5B_2	3.3 (0.69)	6.6
3B_1	3.0 (0.64)	5.1
Average	3.2 (0.67)	5.7

TABLE VI. Bond lengths (\AA) and bond angles (O-Fe-O, in parentheses) of the FeO₂ low-lying two states in this study (GGA and GGA+U), in the linear response calculation (LR⁵⁹), in GGA+U+V (GGA+U+V⁵⁹), in QMC calculation (QMC⁷⁴), and in experimental measurements (Exp.^{75,76})

	GGA	GGA+U	LR	GGA+U+V	QMC	Exp.
5B_2	- (-)	1.64 (115.3°)	1.64 (131°)	1.60 (120°)	- (-)	- (-)
3B_1	1.60 (146.7°)	1.63 (155.8°)	1.67 (180°)	1.58 (156°)	1.59 (156°, 161°)	- (150 ± 10°)

presented the bond length and bond angle after correction by including V (GGA+U+V in Table VI). Since we have not estimated the intersite contribution on the atom-centered orbital basis, it is difficult to judge whether the intersite term is indispensable or not to obtain a better result on the atom-centered orbital basis. However, including the intersite interaction correction might lead to a bond length closer to the QMC result.

D. First-row transition-metal monoxides

We tested three $3d$ transition-metal monoxide molecules, TiO, FeO, and NiO. Diatomic molecules are challenging with the proposed method because their transition-metal d electrons can be considerably displaced in one direction, which can cause substantial errors with the proposed method, as it is based on the atomic likeness of MOs for d electrons and the spherically averaging of U .²⁷ Among the five $3d$ orbitals in the transition-metal atom, under the assumption that the z axis is set as the bonding axis, the two orbitals $d_{x^2} - d_{y^2}$ and d_{xy} are nonbonding orbitals, indicating nearly intact atomic orbitals with high SI energies, while the π bonding MOs of the d_{xz} or the d_{yz} (with ligand p_x or ligand p_y) and the σ bonding MO

of the d_{z^2} (with ligand p_z) are expected to lower calculated U values due to delocalization by hybridization with ligand p orbitals, which can cause deviation from the assumption of the atomic likeness of the MOs for $3d$ electrons.

Table VII shows the calculated U values and related α values for the ground states of the diatomic molecules. The α values were identified to be close to 1, the empirical α value for molecules.³⁷ The U value for NiO $^3\Sigma^-$ is close to that of the linear response, but for the other two cases, TiO $^3\Delta$ and FeO $^5\Delta$, large discrepancies are found between the U values of both methods. This is natural because the two methods adopted different basis sets, and even the same U value can give different geometries and energies. Comparisons of the geometries and energies show the actual effect of these discrepancies in the U values.

In Tables VIII & IX, our bond lengths and dissociation energies for the ground states of the molecules are comparable to those of previous calculations such as the phaseless auxiliary-field quantum Monte Carlo (ph-AFQMC),⁷⁷ CASPT2,⁷⁹ and the linear response method.³² The GGA+U bond lengths look worse than those of the GGA, not to mention those of ph-AFQMC. In our calculations, GGA+U elongates the bond between the transition-metal atom the ligand atom, matching tendency of the linear response results for the ground states of these molecules.³² Given that the GGA bond lengths are already close to the experimental values, elongation scarcely improves the bond length calculation. On the other hand, the GGA+U dissociation energies of TiO and FeO appear to be improved. It appears to be a tendency in our calculations and in the previous linear response calculations³² that GGA+U decreases the dissociation energies of these species, with our GGA dissociation energies being quite large. However, the amounts of reduction of the dissociation energies for FeO and NiO by GGA+U are too large to be similar to the linear response or the experimental values. The poor GGA+U results are likely consequences of the one-direction displacement of transition-metal d electrons and the insufficiency of the basis orbitals. The dissociation energy of TiO (Table IX) is close to the experimental value, most likely because the displaced charge of Ti d electrons is small due to the weak hybridization between the Ti d and O p orbitals. The displaced charges of the Fe d electrons in FeO and the Ni d electrons in NiO must be large, but multiple- ζ basis orbitals or polarization basis orbitals for transition-metal d orbitals may enhance their dissociation energies considerably if the U parameters for these basis orbitals are clearly defined, or one may have to consider another interaction parameter like an intersite interaction parameter V or an on-site interaction U

TABLE VII. The calculated U values of the $3d$ orbitals (eV) for TiO, FeO, and NiO molecules within the proposed method (U^{SIC} . Corresponding α in parentheses) and the previous linear response calculation (LR³²).

	state	U^{SIC}	LR
TiO	$^3\Delta$	3.1 (0.99)	6.03
FeO	$^5\Delta$	4.2 (0.89)	3.01
NiO	$^3\Sigma^-$	4.6 (0.90)	4.34

TABLE VIII. Bond lengths (\AA) of TiO, FeO, and NiO molecules in this study (GGA and GGA+U), in the linear response (LR³²) calculation, in ph-AFQMC calculation (ph-AFQMC⁷⁷), and in experimental measurement (Exp.⁷⁸)

	GGA	GGA+U	LR	ph-AFQMC	Exp.
TiO	1.643	1.650	1.647	1.617	1.620
FeO	1.612	1.678	1.623	1.612	1.616
NiO	1.664	1.688	1.653	1.626	1.627

of another orbital.

IV. DISCUSSION

Our calculations show the deviations to the empirical α value for molecules, *i.e.*, 1. α values close to 1/2 were found in the cases of Fe-porphyrin-CO and FeO₂, while slight

TABLE IX. Calculated dissociation energies (eV) of TiO, FeO, and NiO in this study (GGA and GGA+U), in the linear response calculation (LR³²), in ph-AFQMC with CCSD(T) calculation (ph-AFQMC⁷⁷), in CASPT2 calculation (CASPT2⁷⁹), and in experimental measurement (Exp.⁷⁸)

	GGA	GGA+U	LR	ph-AFQMC	CASPT2	Exp.
TiO	7.89	6.81	6.93	6.98	6.91	6.98
FeO	4.93	3.26	4.35	4.26	4.80	4.22
NiO	4.37	2.92	4.08	4.12	3.85	3.92

deviations from 1 were found for Fe-porphyrin-imidazole and transition-metal monoxides. The results of smaller α values are not less accurate than those of larger α values, although the larger α values are close to the empirical value for molecules. This provides evidence of the necessity of methods to obtain α .

The proposed method can provide calculations comparable to those of hybrid functionals and coupled cluster as well as the linear response method although our method is no match for QMC or CASPT2 in accuracy. Our Fe-porphyrin-imidazole calculation is in good agreement with those of the unrestricted B3LYP and the linear response method. For the cases of Fe-porphyrin-CO and FeO₂, rather good results are given by the proposed method, while our results were not satisfactory for the transition-metal monoxides. The accuracy of our results depends on the molecular geometry and degree of hybridization because suppressing the electron displacement of the target orbital is important during our approximation. If transition-metal d electrons are not considerably displaced, the calculated energies and geometries by the proposed method were close to those calculated by the linear response values or those measured experimentally. On the other hand, incorrect energies could be found in cases with the strong one-direction displacement of transition-metal d electrons. The small displacement of electrons of the target orbital might not be a sufficient condition of our approximation, but it is a necessary condition for atomic likeness of the MO dominated by the target orbital.

One reason those successes is that mapping from SIC reduces the degree of overestimation of the U parameter because the one-orbital SI energy reaches its maximum at the one-electron limit ($\alpha = 1$). Thus, the upper bounds of the effective U values are determined by the SI energies of pure atomic orbitals. Moderate U values can give the reasonable ground state of Fe-porphyrin-CO and the stabilization of the bent structure of FeO₂. Because overestimation of the U values is a type of bias for some cases in the linear response method,¹⁶ suppression of the degree of overestimation makes the proposed method to complement the linear response method. For Fe-porphyrin-CO and FeO₂, the proposed method provides different analyses from those of the linear response method.

A limit of the current version of the proposed method is its use of the single- ζ d orbital in the basis set and its adoption of the Mulliken analysis (and the dual projector). Increasing the basis orbital number can enhance the accuracy of our method, which is influenced by hybridization and polarization. Double- ζ d basis orbitals or polarization orbitals are

necessary for higher accuracy, but this requires a reform of the approximations [Eqs. (14) & (15)], which is left as future work. The Mulliken population scheme has also room for improvement, and there are several suggestions to improve the Mulliken analysis^{80,81} which may serve to modify our method in the future.

We have not applied our method to large-scale molecules of more than a thousand atoms, but application to linear-scaling GGA+U⁸² is necessary because low computational cost is an advantage of the proposed method which has no merits in calculations of small molecules due to insufficient accuracy compared to QMC or CASPT2. Biomolecules are good examples⁸³ to use to test the proposed method. $O(N)$ GGA+U with a U parameter estimated by using our method can be applied to geometry optimization. In our current version of implementation, however, $O(N)$ calculation of the parameter is not available. Linear-scaling version of our method will further reduce computational time. This should be another future task.

V. CONCLUSIONS

We propose a calculation method of the Hubbard U parameter in GGA+U and the α parameter in ASIC for transition-metal d orbitals by mapping SIC onto GGA+U. This method is suitable for atom-centered basis sets, where linear-scaling DFT methods are formulated. The atomic likeness of MOs corresponding to transition-metal d is the key condition of the approximations to reduce the computational cost of finding SI-corrected localized orbitals. SIC can offer a substitute for the Hubbard U parameter in GGA+U, although its usage should be restricted in consideration of difference of GGA+U and SIC. Two assumptions exist here: one-to-one correspondence between a SI-corrected localized orbital and an atomic orbital and the concept of α according to the atomic orbitals. These assumptions lead to the approximate form of the SI-corrected localized orbitals, from which the mapping of SIC onto GGA+U gives the Hubbard U parameter.

The proposed method can provide calculations comparable to the linear response calculations on planewave basis sets, coupled cluster, and hybrid functionals. For the test molecules, the geometries and energies obtained by the method improved over GGA calculations, with some of them even better than the linear response results. Our method does not guarantee better results than the linear response method and hybrid functionals, but mapping from SIC suppresses overestimation of the U parameter. This can provide an alternative analysis

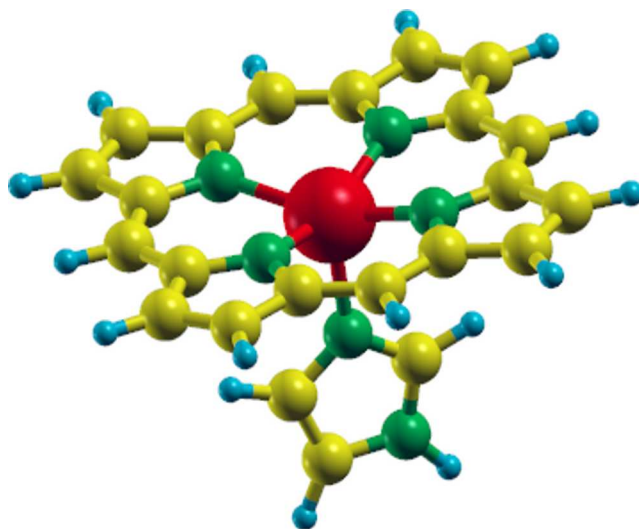


FIG. 1. (Color online). Geometric structure of iron porphyrin imidazole.

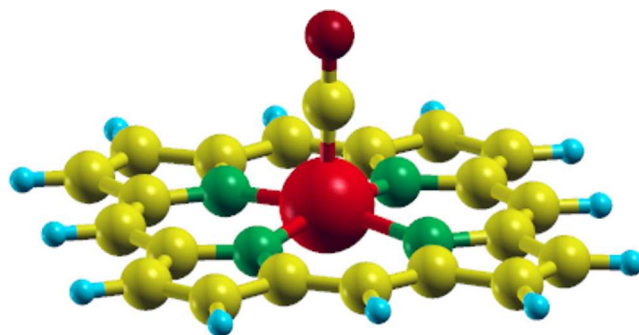


FIG. 2. (Color online). Geometric structure of iron porphyrin carbon monoxide.

of transition-metal complexes.

ACKNOWLEDGMENTS

The author thanks Prof. S.-M. Lee and Prof. M. J. Han for fruitful advices and Mr. E. Sevre for reviewing my manuscript. This work was supported by the Korea Institute of Energy Technology Evaluation and Planning (KETEP) and the Ministry of Trade, Industry & Energy (MOTIE) of the Republic of Korea (No. 20168510030830) and the National Research Foundation of Korea (NRF) grant funded by the Ministry of Science and ICT to SKL (2017R1A2A1A17069511).

REFERENCES

- ¹L. K. McKenzie, H. B. Bryant, and J. A. Weinstein, *Coord. Chem. Rev.* **379**, 2 (2019).
- ²S. Monro, K. L. Colón, H. Yin, J. Roque III, P. Konda, S. Gujar, R. P. Thummel, L. Lilge, C. G. Cameron, and S. A. McFarland, *Chem. Rev.* **119**, 797 (2019).
- ³E. Babu, J. Bhuvaneshwari, P. M. Mareeswaran, P. Thanasekaran, H.-M. Lee, and S. Rajagopal, *Coord. Chem. Rev.* **380**, 519 (2019).
- ⁴C.-N. Ko, G. Li, C.-H. Leung, and D.-L. Ma, *Coord. Chem. Rev.* **381**, 79 (2019).
- ⁵S. K. Nandanwar and H. J. Kim, *ChemistrySelect* **4**, 1706 (2019).
- ⁶Y.-M. Zhao, G.-Q. Yu, F.-F. Wang, P.-J. Wei, and J.-G. Liu, *Chem. Eur. J.* **25**, 3726 (2019).
- ⁷K. E. Dalle, J. Warnan, J. J. Leung, B. Reuillard, I. S. Karmel, and E. Reisner, *Chem. Rev.* **119**, 2752 (2019).
- ⁸R. G. Parr and W. Yang, *Density Functional Theory of Atoms and Molecules* (Oxford University Press, New York, 1989).
- ⁹R. M. Martin, *Electronic Structure: Basic Theory and Practical Methods* (Cambridge University Press, Cambridge, England, 2004).
- ¹⁰J. Kohanoff, *Electronic Structure Calculations for Solids and Molecules* (Cambridge University Press, New York, 2006)
- ¹¹A. Ghosh and P. R. Taylor, *Curr. Opin. Chem. Biol.* **7**, 113 (2003).
- ¹²D. G. Leopold *et al.*, *J. Chem. Phys.* **88**, 3780 (1988).
- ¹³S. Shaik and M. Filatov, *J. Phys. Chem. A* **102**, 3835 (1998).
- ¹⁴C. Rovira *et al.*, *Biophys. J.* **81**, 435 (2001).
- ¹⁵L. Cavallo and H. Jacobsen, *J. Phys. Chem. A* **107**, 5466 (2003).
- ¹⁶D. A. Scherlis, M. Cococcioni, P. Sit, and N. Marzari, *J. Phys. Chem. B* **111**, 7384 (2007).
- ¹⁷M. J. Piotrowski, P. Piquini, L. Cândido, and J. L. F. Da Silva, *Phys. Chem. Chem. Phys.* **13**, 17242 (2011).
- ¹⁸R. Ramakrishnan, A. V. Matveev, and N. Rösch, *Chem. Phys. Lett.* **468**, 158 (2009).
- ¹⁹M. J. Han, T. Ozaki, and J. Yu, *Chem. Phys. Lett.* **492**, 89 (2010).
- ²⁰A. D. Becke, *J. Chem. Phys.* **98**, 5648 (1993).
- ²¹M.-S. Liao, J. D. Watts, and M.-J. Huang, *J. Comput. Chem.* **27**, 1577 (2006).
- ²²H. J. Kulik, M. Cococcioni, D. A. Scherlis, and N. Marzari, *Phys. Rev. Lett.* **97**, 103001

- (2006).
- ²³H. J. Kulik, J. Chem. Phys. **142**, 240901 (2015).
- ²⁴V. I. Anisimov, F. Aryasetiawan, and A. I. Lichtenstein, J. Phys.: Condens. Matter **9**, 767 (1997).
- ²⁵M. J. Han, T. Ozaki, and J. Yu, Phys. Rev. B **73**, 045110 (2006).
- ²⁶B. Himmetoglu, A. Floris, S. de Gironcoli, and M. Cococcioni, Int. J. Quantum Chem. **114**, 14 (2014).
- ²⁷S. L. Dudarev, G. A. Botton, S. Y. Savrasov, C. J. Humphreys, and A. P. Sutton, Phys. Rev. B **57**, 1505 (1998).
- ²⁸W. E. Pickett, S. C. Erwin, and E. C. Ethridge, Phys. Rev. B **58**, 1201 (1998).
- ²⁹M. Cococcioni and S. de Gironcoli, Phys. Rev. B **71**, 035105 (2005).
- ³⁰H. Hsu, K. Umemoto, M. Cococcioni, and R. M. Wentzcovitch, Phys. Rev. B **79**, 125124 (2009).
- ³¹H. Hsu, P. Blaha, M. Cococcioni, and R. M. Wentzcovitch, Phys. Rev. Lett. **106**, 118501 (2011).
- ³²H. J. Kulik and N. Marzari, J. Chem. Phys. **133**, 114103 (2010).
- ³³W.-J. Lee and Y.-S. Kim, J. Korean Phys. Soc. **60**, 781 (2012).
- ³⁴Q. Zhao, E. I. Ioannidis, and H. J. Kulik, J. Chem. Phys. **145**, 054109 (2016).
- ³⁵E. B. Linscott, D. J. Cole, M. C. Payne, and D. D. O'Regan, Phys. Rev. B **98**, 235157 (2018).
- ³⁶J. P. Perdew and A. Zunger, Phys. Rev. B **23**, 5048 (1981).
- ³⁷C. D. Pemmaraju, T. Archer, D. Sánchez-Portal, and S. Sanvito, Phys. Rev. B **75**, 045101 (2007).
- ³⁸J. G. Harrison, R. A. Heaton, and C. C. Lin, J. Phys. B **16**, 2079 (1983).
- ³⁹M. R. Pederson, R. A. Heaton, and C. C. Lin, J. Chem. Phys. **80**, 1972 (1984).
- ⁴⁰M. R. Pederson, R. A. Heaton, and C. C. Lin, J. Chem. Phys. **82**, 2688 (1985).
- ⁴¹A. Zunger, Phys. Rev. B **22**, 649 (1980).
- ⁴²M. M. Rieger and P. Vogl, Phys. Rev. B **52**, 16567 (1995).
- ⁴³D. Vogel, P. Krüger, and J. Pollmann, Phys. Rev. B **54**, 5495 (1996).
- ⁴⁴D. Vogel, P. Krüger, and J. Pollmann, Phys. Rev. B **55**, 12836 (1997).
- ⁴⁵A. Filippetti and N. A. Spaldin, Phys. Rev. B **67**, 125109 (2003).
- ⁴⁶A. Filippetti and V. Fiorentini, Eur. Phys. J. B **71**, 139-183 (2009).

- ⁴⁷I. V. Solovyev and P. H. Dederichs, *Phys. Rev. B* **49**, 6736 (1994).
- ⁴⁸I. G. Austin and N. F. Mott, *Science* **168**, 71 (1970).
- ⁴⁹W. R. Scheidt and C. A. Reed, *Chem. Rev.* **81**, 543 (1981).
- ⁵⁰T. Ozaki and H. Kino, *Phys. Rev. B* **69**, 195113 (2004).
- ⁵¹One should consider numerical errors in application of the condition of inequality.
- ⁵²J. M. Soler, E. Artacho, J. D. Gale, A. Garcia, J. Junquera, P. Ordejon, and D. Sanchez-Portal, *J. Phys.: Condens. Matter* **14**, 2745 (2002).
- ⁵³J. P. Perdew, K. Burke, M. Ernzerhof, *Phys. Rev. Lett.* **77**, 3865 (1996).
- ⁵⁴<http://openmx-square.org>
- ⁵⁵N. Troullier and J. L. Martins, *Phys. Rev. B* **43**, 1993 (1991).
- ⁵⁶P. E. Blochl, *Phys. Rev. B* **41**, 5414 (1990).
- ⁵⁷S. G. Louie, S. Froyen, and M. L. Cohen, *Phys. Rev. B* **26**, 1738 (1982).
- ⁵⁸S. F. Boys and F. Bernardi, *Mol. Phys.* **19**, 553 (1970).
- ⁵⁹H. J. Kulik, N. Marzari, *J. Chem. Phys.* **134**, 094103 (2011).
- ⁶⁰Md. E. Ali, B. Sanyal, and P. M. Oppeneer, *J. Phys. Chem. B* **116**, 5849 (2012).
- ⁶¹M. Radoń, *J. Chem. Theory Comput.* **10**, 2306 (2014).
- ⁶²J. Vojtěchovský, K. Chu, J. Berendzen, R. M. Sweet, I. Schlichting, *Biophys. J.* **77**, 2153 (1999).
- ⁶³M. Momenteau, W. R. Scheidt, C. W. Eigenbrot, C. A. Reed, *J. Am. Chem. Soc.* **110**, 1207 (1998).
- ⁶⁴G. B. Jameson, F. Molinaro, J. A. Ibers, J. P. Collman, J. I. Brauman, E. Rose, K. S. Suslick, *J. Am. Chem. Soc.* **102**, 3224 (1980).
- ⁶⁵K. S. Suslick, C. T. Chen, M. E. Kosal, J.-H. Chou, *J. Porphyrins Phthalocyanines* **4**, 407 (2007); H. Nakanishi, K. Miyamoto, M. Y. Davis, E. S. Dy, R. Tanaka, and H. Kasai, *J. Phys.: Condens. Matter* **19**, 365234 (2007).
- ⁶⁶C. Rovira, P. Ballone, and M. Parrinello, *Chem. Phys. Lett.* **271**, 247 (1997).
- ⁶⁷M.-S. Liao, J. D. Watts, and M.-J. Huang, *J. Phys. Chem. A* **109**, 7988 (2005).
- ⁶⁸T. Ohta, B. Pal, and T. Kitagawa, *J. Phys. Chem. B* **109**, 21110 (2005).
- ⁶⁹T. Karpuschkin, M. M. Kappes, and O. Hampe, *Angew. Chem. Int. Ed.* **52**, 10374 (2013).
- ⁷⁰A. Altun, M. Saitow, F. Neese, and G. Bistoni, *J. Chem. Theory Comput.* **15**, 1616 (2019).
- ⁷¹T. E. Shubina and T. Clark, *J. Coord. Chem.* **63**, 2854 (2010).
- ⁷²M. Radoń and K. Pierloot, *J. Phys. Chem. A* **112**, 11824 (2008).

- ⁷³S.-M. Peng and J.A. Ibers, *J. Am. Chem. Soc.* **25**, 8032 (1976).
- ⁷⁴L. K. Wagner, *J. Chem. Phys.* **138**, 094106 (2013).
- ⁷⁵G. Chertihin, W. Saffel, J. Yustein, L. Andrews, M. Neurock, A. Ricca, and C. Bauschlicher, *J. Phys. Chem.* **100**, 5261 (1996).
- ⁷⁶L. Andrews, G. Chertihin, A. Ricca, and C. Bauschlicher, *J. Am. Chem. Soc.* **118**, 467 (1996).
- ⁷⁷J. Shee, B. Rudshiteyn, E. J. Arthur, S. Zhang, D. R. Reichman, and R. A. Friesner, *J. Chem. Theory Comput.* **15**, 2346 (2019).
- ⁷⁸J. F. Harrison, *Chem. Rev.* **100**, 679 (2000).
- ⁷⁹J. L. Bao, S. M. Odoh, L. Gagliardi, and D. G. Truhlar, *J. Chem. Theory Comput.* **13**, 616 (2017).
- ⁸⁰F. M. Bickelhaupt, N. J. R. van Eikema Hommes, C. F. Guerra, and E. J. Baerends, *Organometallics* **15**, 2923 (1996).
- ⁸¹S. Tiwari, P. K. Shukla, and P. C. Mishra, *J. Mol. Model* **14**, 631 (2008).
- ⁸²D. J. Cole, D. D. O'Regan, and M. C. Payne, *J. Phys. Chem. Lett.* **3**, 1448 (2012).
- ⁸³D. J. Cole and N. D. M. Hine, *J. Phys.: Condens. Matter* **28**, 393001 (2016).